

Laser influence on positron-antiproton radiative capture collision

 S.-M. Li^{1,2,a}, Z.-J. Chen³, Q.-Q. Wang², and Z.-F. Zhou²
¹ Chinese Center of Advanced Science and Technology (World Laboratory), P.O. Box 8730, Beijing 100080, People's Republic of China

² Department of Modern Physics, University of Science and Technology of China, P.O. Box 4, Hefei, Anhui 230027, People's Republic of China

³ Department of Physics, Anhui University, Hefei, Anhui 230039, People's Republic of China

Received: 13 November 1998 / Received in final form: 16 March 1999

Abstract. The laser-assisted radiative capture between a positron and an antiproton is studied in detail. The theoretical results show that the cross-section for antihydrogen formation is significantly reduced with the application of a laser background. This effect is most marked when the laser polarization is parallel to the incident direction.

PACS. 34.50.Rk Laser-modified scattering and reactions – 34.70.+e Charge transfer – 32.80.Wr Other multiphoton processes

1 Introduction

When two oppositely charged particles collide with each other, bound states between them may form through radiative recombination. However, such a recombination process is extremely difficult; a small disturbance to the state of either of the colliders may destroy the bound-state formation. For instance, if this reaction is placed in a laser background, the probability of bound-state formation may be reduced remarkably [1]. In this article, we will investigate the influence of a laser on one of the simplest radiative capture collisions,

$$e^+ + \bar{p} \longrightarrow \bar{H} + \hbar\omega, \quad (1.1)$$

Such a process, in a laser-free environment, can occur in the trapped plasma of antiprotons and positrons or in the collision between two beams of them [2, 3]. In Section 2 we give the S -matrix and the scattering amplitudes for each partial wave. In Section 3 we discuss the laser-modified cross-sections, and the dependence of the results on laser strength, frequency, polarization direction, etc. Section 4 contains conclusions.

2 Theory

Let us consider the laser-assisted capture reaction (1.1) between a positron and an antiproton. During this process, L photons may be exchanged between the laser background and the positron-antiproton system. If we denote the impact energy of the positron by E , the ground-state energy

of final-state antihydrogen by $W_0^{\bar{H}}$, the laser photon energy by $\hbar\omega_0$, and the emitted photon energy in final state by $\hbar\omega$, then we have

$$\hbar\omega = E + L\hbar\omega_0 - W_0^{\bar{H}}. \quad (2.1)$$

We will assume that the laser field is treated classically as a spatially homogeneous electric field, linearly polarized, and single model,

$$\varepsilon = \varepsilon_0 \sin \omega_0 t. \quad (2.2)$$

For the nonrelativistic case, the S -matrix element for the laser-assisted positron-antiproton radiative capture into the dressed ground state of antihydrogen (in the atomic units $\hbar = e = m = 1$) is

$$S = -i \int_{-\infty}^{\infty} dt \langle \psi_F(\mathbf{r}, t) | \mathbf{a} \cdot \nabla e^{-i(\mathbf{k} \cdot \mathbf{r} - \omega t)} | \chi_I(\mathbf{r}, t) \rangle \quad (2.3)$$

in which \mathbf{a} is the polarization vector of the final photon state [4]. Here we have neglected the laser effect on the antiproton because it is much heavier than the positron. χ_I is the laser-modified wave function of the incident positron [5, 6],

$$\begin{aligned} \chi_I(\mathbf{r}, t) = & (2\pi)^{-3/2} e^{\pi\xi/2} \Gamma(1 - i\xi) F(i\xi, 1, i(pr - \mathbf{p} \cdot \mathbf{r})) \\ & \times \exp \left[i(\mathbf{p} \cdot \mathbf{r} + \mathbf{p} \cdot \alpha_0 \sin \omega_0 t - Et) - \frac{i}{2c^2} \right. \\ & \left. \times \int_{-\infty}^t dt' A^2(t') \right] \end{aligned} \quad (2.4)$$

with $\xi = 1/137p$, $E = p^2/2$, $\alpha_0 = \varepsilon_0/\omega_0^2$, and $F(i\xi, 1, i(pr - \mathbf{p} \cdot \mathbf{r}))$ is the confluent hypergeometrical function. ψ_F is the dressed ground state of antihydrogen in the

^a e-mail: lism@ustc.edu.cn

soft-photon approximation (see the Appendix),

$$\psi_F(\mathbf{r}, t) = \exp \left[-iW_0^{\bar{H}}t - \frac{i}{2c^2} \int_{-\infty}^t dt' A^2(t') \right] \times \left(1 + \frac{i}{\omega_0} \varepsilon_0 \cdot \mathbf{r} \cos \omega_0 t \right) \phi_0^{\bar{H}}(\mathbf{r}), \quad (2.5)$$

where

$$\phi_0^{\bar{H}}(\mathbf{r}) = \sqrt{\frac{\eta^3}{\pi}} e^{-\eta r} (\eta = 1) \quad (2.6)$$

is the ground-state wave function of antihydrogen. In equation (2.5) the term $\frac{i}{\omega_0} \varepsilon_0 \cdot \mathbf{r} \cos \omega_0 t$ is responsible for the laser modification on the antihydrogen state. This indicates that the laser “stretches” the positron cloud in the polarization direction. The stronger the laser, the more the positron cloud is stretched; the lower the field frequency, the more the positron deviates from its ground state. Because the factor $\exp[-\frac{i}{2c^2} \int_{-\infty}^t dt' A^2(t')]$ is exactly the same in both the initial state of equation (2.4) and the final state of equation (2.5), it will be cancelled in the S -matrix of equation (2.3). Then the time integration in equation (2.3) can be readily performed by using the generating function for Bessel functions

$$e^{iy \sin u} = \sum_{L=-\infty}^{\infty} J_L(y) e^{iLu} \quad (2.7)$$

and the formula

$$J_{L+1}(y) + J_{L-1}(y) = \frac{2L}{y} J_L(y). \quad (2.8)$$

The result is

$$S = -i \sum_{L=-\infty}^{\infty} f_L \delta(E - W_0 - \omega - L\omega_0), \quad (2.9)$$

where

$$f_L = N J_L(\mathbf{p} \cdot \alpha_0) \left(M + \frac{L}{\mathbf{p} \cdot \alpha_0} \widetilde{M} \right) \quad (2.10)$$

in which $N = \sqrt{\eta^5/\pi} e^{\pi\xi/2} \Gamma(1 - i\xi)$, and

$$M = \int d^3r \frac{\mathbf{a} \cdot \mathbf{r}}{r} e^{i(\mathbf{p}-\mathbf{k}) \cdot \mathbf{r} - \eta r} F(i\xi, 1, i(pr - \mathbf{p} \cdot \mathbf{r})), \quad (2.11)$$

$$\widetilde{M} = \frac{i}{\omega_0} \int d^3r \left[\varepsilon_0 \cdot \mathbf{a} - (\varepsilon_0 \cdot \mathbf{r}) \frac{\mathbf{a} \cdot \mathbf{r}}{r} \right] \cdot e^{i(\mathbf{p}-\mathbf{k}) \cdot \mathbf{r} - \eta r} F(i\xi, 1, i(pr - \mathbf{p} \cdot \mathbf{r})). \quad (2.12)$$

Equations (2.9) and (2.10) show that the S -matrix is decomposed into many partial waves due to the laser modification to the state of the incident positron. The amplitude for each partial wave is proportional to a Bessel function related to the incident momentum and laser strength. The

integrals in equations (2.11) and (2.12) can be evaluated with the help of the following formula [4, 7]:

$$\int d^3r \frac{e^{i(\mathbf{p}-\mathbf{k}) \cdot \mathbf{r} - \eta r}}{r} F(i\xi, 1, i(pr - \mathbf{p} \cdot \mathbf{r})) = 4\pi \frac{[k^2 + (\eta - ip)^2]^{-i\xi}}{[(\mathbf{p} - \mathbf{k})^2 + \eta^2]^{1-i\xi}}. \quad (2.13)$$

It is easy to show by differentiating under the integral sign that

$$M = 8\pi i (1 - i\xi) (\mathbf{a} \cdot \mathbf{p}) \frac{[k^2 + (\eta - ip)^2]^{-i\xi}}{[(\mathbf{p} - \mathbf{k})^2 + \eta^2]^{2-i\xi}}, \quad (2.14)$$

$$\begin{aligned} \widetilde{M} &= -\frac{4\pi i}{\omega_0} (\varepsilon_0 \cdot \mathbf{a}) \frac{\partial}{\partial \eta} \frac{[k^2 + (\eta - ip)^2]^{-i\xi}}{[(\mathbf{p} - \mathbf{k})^2 + \eta^2]^{1-i\xi}} \\ &+ \frac{8\pi i}{\omega_0} (1 - i\xi) (\mathbf{a} \cdot \mathbf{p}) \varepsilon_0 \cdot \frac{\partial}{\partial \mathbf{k}} \frac{[k^2 + (\eta - ip)^2]^{-i\xi}}{[(\mathbf{p} - \mathbf{k})^2 + \eta^2]^{2-i\xi}}. \end{aligned} \quad (2.15)$$

In writing the above formula, we have taken into account $\mathbf{a} \cdot \mathbf{k} = 0$.

Summing over the emitted photon polarization in the final state, we can write the differential cross-section of the laser-assisted process (1.1) for each partial wave corresponding to L soft photons exchanged between the collision system and the laser field,

$$\frac{d\sigma_L}{d\Omega} = \frac{\omega}{2(2\pi)^2 v} \overline{|f_L|^2} = \frac{\omega}{8\pi^2 p} \overline{|f_L|^2}, \quad (2.16)$$

where $v = p$ is the velocity of the incident positron, and $\overline{|f_L|^2}$ represents an average of $|f_L|^2$ over all emitted photon polarizations \mathbf{a} [4]. The cross-section of antihydrogen formation is the sum of all the partial cross-sections,

$$\frac{d\sigma}{d\Omega} = \sum_{L=-\infty}^{\infty} \frac{d\sigma_L}{d\Omega}. \quad (2.17)$$

3 Results and discussion

In Figure 1 we display the differential cross-section of the laser-assisted reaction (1.1) at an azimuth angle $\varphi = 0^\circ$ (we set the z -axis of the coordinate system along the positron incident direction, and assume that the electric vector of the laser field is in the xOz plane) for impact energy $E = 10$ eV, with field strength $\varepsilon_0 = 10^8$ V/cm, and frequency $\hbar\omega = 1.17$ eV. The theoretical results show that for a geometry in which the laser polarization is set parallel or antiparallel to the incident direction $\varepsilon_0 \parallel \mathbf{k}_I$, the cross-section is greatly lowered (solid line). For a laser polarization geometry perpendicular to the incident direction $\varepsilon_0 \perp \mathbf{k}_I$, the result at small and large scattering angles is increased (short-dashed line). At intermediate angles the laser-modified cross-section is nearly indistinguishable from the result in the absence of the laser (long-dashed line). As a matter of fact, the radiative capture process is extremely unstable, a small disturbance from the laser

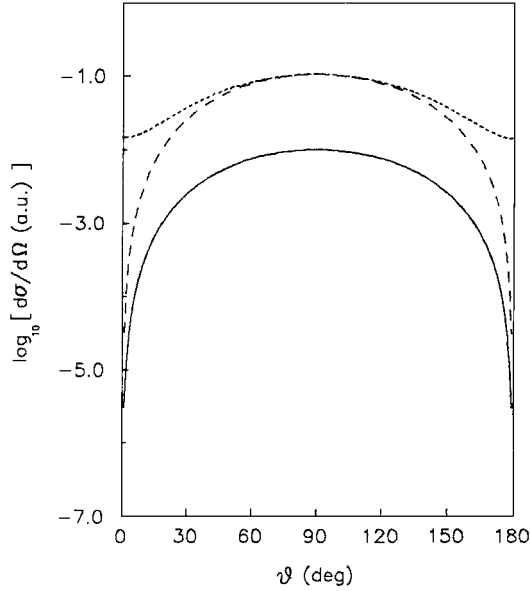


Fig. 1. Differential cross-sections of emitted photons against the scattering angle θ at azimuth angle $\varphi = 0^\circ$ for the laser-assisted radiative capture $e^+ + \bar{p} \rightarrow \bar{H}(1s) + \hbar\omega$ at positron energy $E = 10$ eV, laser strength $\varepsilon_0 = 10^8$ V/cm, and frequency $\hbar\omega_0 = 1.17$ eV. Solid line: result for a parallel geometry $\varepsilon_0 \parallel \mathbf{k}_I$. Short-dashed line: result for a perpendicular geometry $\varepsilon_0 \perp \mathbf{k}_I$. Long-dashed line: laser-free result.

may destroy such a capture process, thus the probability of antihydrogen formation is significantly reduced in general. For a perpendicular geometry, the laser leads to a small vertical vibration of the positron and hence increases the probability of the positron to “meet” with the target as it passes by. This causes the capture cross-section to be slightly increased. Figure 2 gives the dependence of the differential cross-section on the azimuthal angle for a perpendicular geometry $\varepsilon_0 \parallel \mathbf{k}_I$. We find that it is not sensitive to the azimuthal angle.

Figure 3 exhibits the total radiative capture cross-sections. All these results drop rapidly with increasing impact energy. When the laser polarization is set in a parallel geometry to the incident positron, the total cross-section is remarkably reduced. The higher the impact energy, the more difficult it is to form a bound state, thus the more noticeably the cross-section is lowered. The cross-section for a perpendicular geometry is slightly increased at low energy where laser polarization gives noticeable contributions. With increasing energy, the laser modification of the positron trajectory is too small to affect the total cross-section. Both curves merge into one.

Figure 4 demonstrates the total cross-section for each soft photon number L . We find that the contributions of photon absorption ($L < 0$) and emission ($L > 0$) are roughly symmetric. Only those L values contained in a certain range have significant contributions.

Figure 5 illustrates the dependence of the total cross-section on field strength in the case of parallel geometry. The figure shows that at low laser intensities, the effect of the laser is unimportant. When the field strength in-

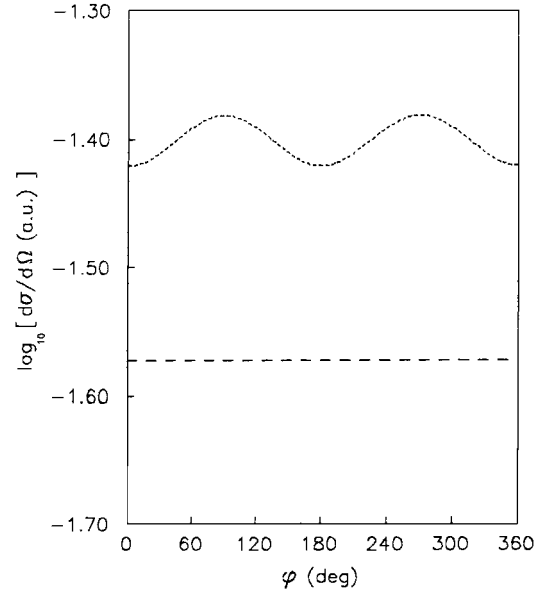


Fig. 2. Differential cross-section against the azimuth angle φ at scattering angle $\theta = 30^\circ$ for a perpendicular geometry $\varepsilon_0 \perp \mathbf{k}_I$ with $E = 10$ eV, $\varepsilon_0 = 10^8$ V/cm, and $\hbar\omega_0 = 1.17$ eV. Short-dashed line: result with laser modification. Long-dashed line: laser-free result.

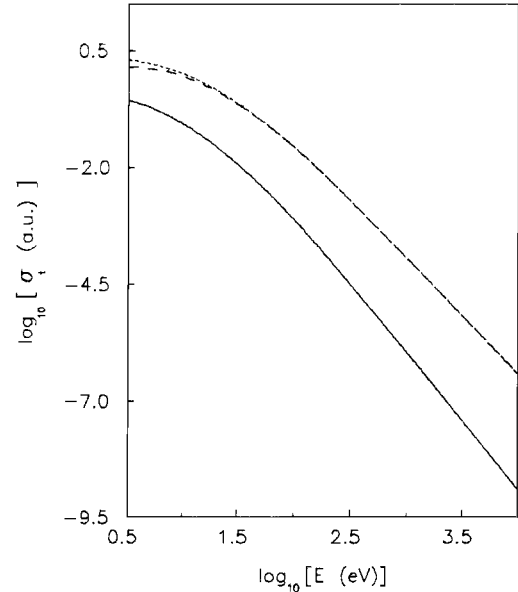


Fig. 3. Total radiative capture cross-section for $\varepsilon_0 = 10^8$ V/cm and $\hbar\omega_0 = 1.17$ eV. Solid line: result for $\varepsilon_0 \parallel \mathbf{k}_I$. Short-dashed line: result for $\varepsilon_0 \perp \mathbf{k}_I$. Long-dashed line: laser-free result.

creases up to a certain value, the cross-section decreases rapidly and is accompanied by oscillations. Figure 6 indicates that the cross-section dependence on laser frequency is opposite: the lower the frequency, the more the cross-section is lowered. At high frequency, the effect of the laser reaches saturation. In fact, the lower the frequency, the more markedly the positron is polarized in the incident direction, thus the more the cross-section is reduced. Otherwise if the laser frequency becomes higher and higher,

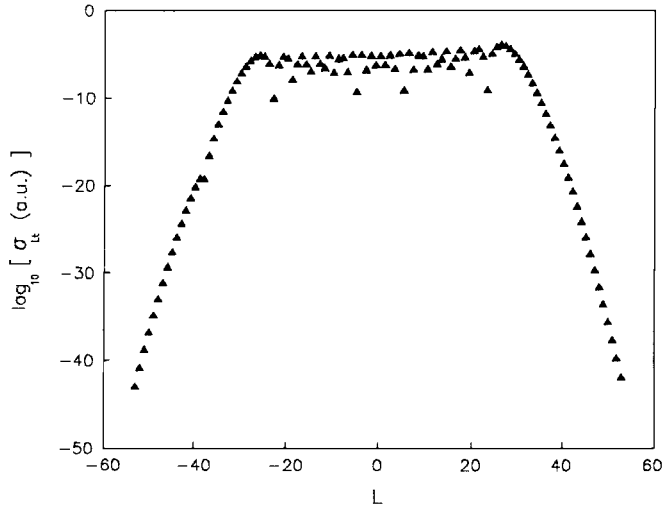


Fig. 4. Total cross-section for each number of soft photons exchanged between the scattering system and the laser background for a parallel geometry with $E = 100$ eV, $\varepsilon_0 = 10^8$ V/cm, and $\hbar\omega_0 = 1.17$ eV ($L < 0$ represents photon emission; $L > 0$ photon absorption).

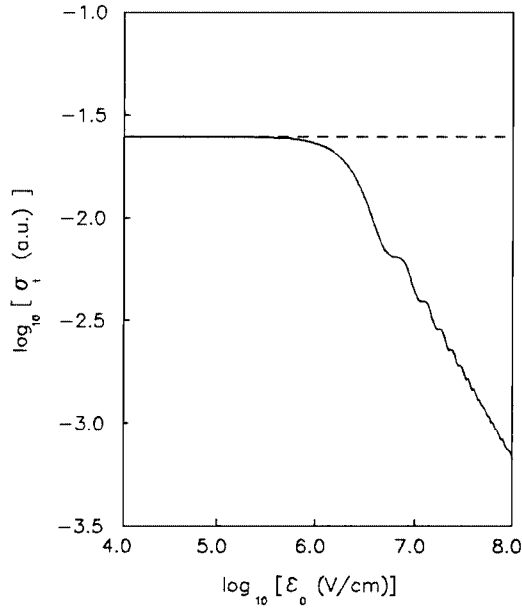


Fig. 5. The dependence of the total cross-section on laser strength at $\hbar\omega_0 = 1.17$ eV and $E = 100$ eV. Solid line: result for a parallel geometry. Dashed line: laser-free result.

the positron can hardly respond so rapidly to the laser oscillation, and the average dressing effect on the cross-section is omissible. Figure 7 describes the cross-section dependence on the polarization direction. The more the polarization approaches the parallel direction, the smaller the cross-section. With increasing polarization angle, the result increases with many small oscillations. As the polarization turns up to a perpendicular geometry, the cross-section reaches its maximum. The oscillations present in these figures are mainly caused by the Bessel function

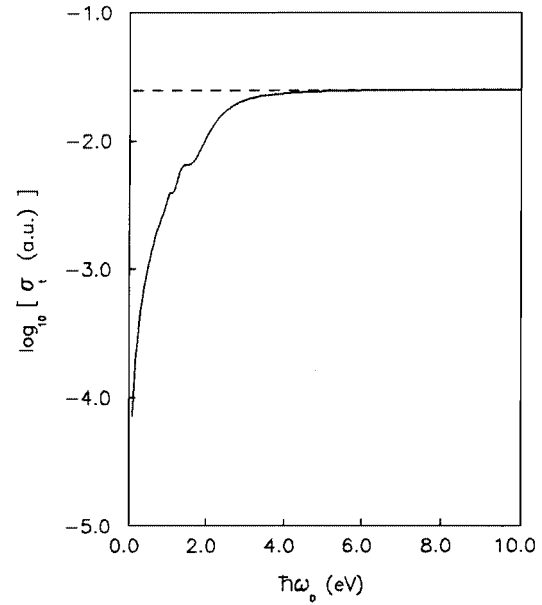


Fig. 6. Total cross-section against laser frequency for $\varepsilon_0 = 10^7$ V/cm, and $E = 100$ eV. Solid line: result for a parallel geometry. Dashed line: laser-free result.

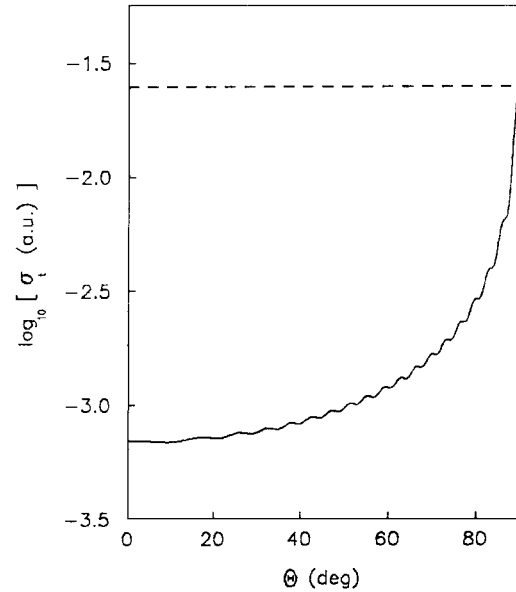


Fig. 7. The dependence of the total cross-section on laser polarization direction (the electric vector varies in the xOz plane) for $E = 100$ eV, $\varepsilon_0 = 10^8$ V/cm, and $\hbar\omega_0 = 1.17$ eV. Solid line: laser present. Dashed line: laser-free result.

$J_L(\mathbf{p} \cdot \alpha_0)$ in equation (2.10). Because each component in the spectrum varies with the field strength and polarization in different ways, their contribution to the cross-section sum is not synchronous with the scattering angle increase. This is responsible for the oscillations shown in these figures.

4 Conclusions

We have presented a detailed investigation into the positron-antiproton radiative capture collision in the presence of a laser field. The laser-modified wave function of the positron is given, taking into account the Coulomb boundary condition. The wave function of a dressed atom is improved compared to that in preceding works (see the Appendix). The laser modification of the radiative capture cross-section and its dependence on laser field strength, frequency, and polarization direction are discussed.

In comparison with other laser-assisted electron capture processes between ions and atoms in which the cross-section is mostly increased by a laser field [8–10], the cross-section for laser-assisted radiative capture scattering in most cases is lowered except for the perpendicular geometry. Thus it is not practical to use a laser to improve the efficiency of antihydrogen production in a radiative capture collision. On the contrary, one may reduce the extent of radiative capture with the application of a laser background. The same mechanism applies to the electron-positron collision or the collisions between oppositely charged light and heavy particles.

This work is supported by the Returned Student Foundation of Academia Sinica, the Start Foundation for Returned Students of University of Science and Technology of China, and the Chinese Research for Atomic and Molecular Data. Dr. Murry Sherk read the manuscript.

Appendix: The dressed wave function of an atom embedded in a laser field

Supposing that the electric vector of a laser field is given by equation (2.2), the corresponding vector potential is

$$\mathbf{A} = \mathbf{A}_0 \cos \omega_0 t \quad (\text{A.1})$$

with $\mathbf{A}_0 = c\varepsilon_0/\omega_0$, here c is the velocity of light in vacuum. The dressed states of an atom embedded in such a field can be obtained by solving the coupled Schrödinger equation (in the usual units)

$$i\hbar \frac{\partial}{\partial t} \psi(\mathbf{r}_1, \dots, \mathbf{r}_Z, t) = \left\{ \frac{1}{2m} \sum_{j=1}^Z \left[\hat{p}_j + \frac{e}{c} \mathbf{A}(t) \right]^2 + V(\mathbf{r}_1, \dots, \mathbf{r}_Z) \right\} \times \psi(\mathbf{r}_1, \dots, \mathbf{r}_Z, t), \quad (\text{A.2})$$

where Z is the atomic number, and \mathbf{r}_j ($j = 1, \dots, Z$) denotes the coordinate of the j -th electron of the atom. Performing the gauge transformation

$$\psi(\mathbf{r}_1, \dots, \mathbf{r}_Z, t) = \exp \left[-i \frac{Ze^2}{2mc^2\hbar} \int_{-\infty}^t dt' A^2(t') \right] \psi'(\mathbf{r}_1, \dots, \mathbf{r}_Z, t), \quad (\text{A.3})$$

we obtain

$$i\hbar \frac{\partial}{\partial t} \psi'(\mathbf{r}_1, \dots, \mathbf{r}_Z, t) = \left\{ \frac{1}{2m} \sum_{j=1}^Z \hat{p}_j^2 + \frac{e}{mc} \mathbf{A}(t) \cdot \sum_{j=1}^Z \hat{p}_j + V(\mathbf{r}_1, \dots, \mathbf{r}_Z) \right\} \times \psi'(\mathbf{r}_1, \dots, \mathbf{r}_Z, t). \quad (\text{A.4})$$

We shall assume that the corresponding undressed Schrödinger equation is exactly solvable, and the second term in (A.4) may be treated as a time-dependent perturbation (*i.e.* $|eA_0/(c\sqrt{mW})| \sim |e\varepsilon_0/(\omega\sqrt{mW})| \ll 1$, W is the bound energy of the atom with laser absent). Then the new Schrödinger equation (A.4) is readily solved by using time-dependent perturbation theory. Suppose that the atom is initially at the state ϕ_n . Then the dressed wave function to the first order in the soft-photon approximation is given by [11]

$$\begin{aligned} \psi'_n(\mathbf{r}_1, \dots, \mathbf{r}_Z, t) &= e^{-\frac{i}{\hbar} W_n t} \left\{ \phi_n(\mathbf{r}_1, \dots, \mathbf{r}_Z) - \frac{1}{2\hbar} \right. \\ &\times \sum_{m \neq n} \left[\frac{e^{i\omega_0 t}}{\omega_{mn} + \omega_0} + \frac{e^{-i\omega_0 t}}{\omega_{mn} - \omega_0} \right] \\ &\times \left\langle m \left| \frac{e}{mc} \mathbf{A}_0 \cdot \sum_{j=1}^Z \hat{\mathbf{p}}_j \right| n \right\rangle \phi_m(\mathbf{r}_1, \dots, \mathbf{r}_Z) \left. \right\} \\ &\approx e^{-\frac{i}{\hbar} W_n t} \left\{ \phi_n(\mathbf{r}_1, \dots, \mathbf{r}_Z) - \frac{e}{\hbar mc} \mathbf{A}_0 \cos \omega_0 t \cdot \sum_{m \neq n} \frac{1}{\omega_{mn}} \right. \\ &\times \left\langle m \left| \sum_{j=1}^Z \hat{\mathbf{p}}_j \right| n \right\rangle \phi_m(\mathbf{r}_1, \dots, \mathbf{r}_Z) \left. \right\}, \quad (\text{A.5}) \end{aligned}$$

where $\omega_{mn} = (E_m - E_n)/\hbar$ is the Bohr frequency of the atom. In treating the sum term in equation (A.5), an average excitation approximation is generally used to simplify the computation in preceding works [11–14]. Here we find that such an approximation is unnecessary, and the precision of the dressed wave function may be improved. In fact, by using the relation $[x_i, p_j] = i\hbar\delta_{ij}$, it is easy to show that

$$\sum_{m \neq n} \frac{1}{\omega_{mn}} |m\rangle \langle m| \hat{\mathbf{p}}_j |n\rangle = \frac{im}{\hbar} \mathbf{r}_j |n\rangle. \quad (\text{A.6})$$

The wave function of (A.5) is then reduced to

$$\begin{aligned} \psi'_n(\mathbf{r}_1, \dots, \mathbf{r}_Z, t) &\approx e^{-\frac{i}{\hbar} W_n t} \\ &\times \left\{ 1 - \frac{ie}{\hbar^2 c} \mathbf{A}_0 \cos \omega_0 t \cdot \sum_{j=1}^Z \mathbf{r}_j \right\} \phi_n(\mathbf{r}_1, \dots, \mathbf{r}_Z) = \\ &e^{-\frac{i}{\hbar} W_n t} \left(1 - \frac{ie}{\hbar^2 \omega_0} \varepsilon_0 \cos \omega_0 t \cdot \sum_{j=1}^Z \mathbf{r}_j \right) \\ &\times \phi_n(\mathbf{r}_1, \dots, \mathbf{r}_Z). \quad (\text{A.7}) \end{aligned}$$

Substituting this into (A.3), we finally obtain the approximate wave function of the dressed atom,

$$\begin{aligned} \psi_n(\mathbf{r}_1, \dots, \mathbf{r}_Z, t) \approx & \\ \exp \left[-\frac{i}{\hbar} W_n t - i \frac{Ze^2}{2mc^2 \hbar} \int_{-\infty}^t dt' A^2(t') \right] & \\ \times \left(1 - \frac{ie}{\hbar^2 \omega_0} \varepsilon_0 \cos \omega_0 t \cdot \sum_{j=1}^Z \mathbf{r}_j \right) \phi_n(\mathbf{r}_1, \dots, \mathbf{r}_Z). \end{aligned} \quad (\text{A.8})$$

For the dressed states of an antihydrogen atom, we can simply set $Z = 1$, and reverse the sign of charge.

References

1. S.-M. Li, Y.-G. Miao, Z.-F. Zhou, J. Chen, Y.-Y. Liu, Phys. Rev. A **58**, 2615 (1998).
2. G. Gabrielse, S. L. Rolston, L. Haarsma, Phys. Lett. A **129**, 38 (1988).
3. M. Charlton, J. Eades, D. Horváth, R.J. Hughes, C. Zimmermann, Phys. Rep. **241**, 65 (1994).
4. A.I. Akhiezer, N.P. Merenkov, J. Phys. B: At. Mol. Opt. Phys. **29**, 2135 (1996).
5. M. Jain, N. Tzoar, Phys. Rev. A **18**, 538 (1978).
6. P. Cavaliere, G. Ferrante, C. Leone, J. Phys. B: At. Mol. Phys. **13**, 4495 (1980).
7. A.I. Akhiezer, V.B. Berestetsky, *Quantum Electrodynamics* (Nauka, Moscow, 1969).
8. S.-M. Li, Y.-G. Miao, Z.-F. Zhou, J. Chen, Y.-Y. Liu, Z. Phys. D **39**, 29 (1997).
9. S.-M. Li, X.-L. Xu, Z.-F. Zhou, J. Chen, Y.-Y. Liu, Eur. Phys. J. D **2**, 237 (1998).
10. S.-M. Li, Y.-G. Miao, Z.-F. Zhou, J. Chen, Y.-Y. Liu, Phys. Rev. A **57**, 3705 (1998).
11. S.-M. Li, Z.-F. Zhou, J.-G. Zhou, Y.-Y. Liu, Phys. Rev. A **47**, 4960 (1993).
12. M. Bhattacharya, C. Sinha, N.C. Sil, Phys. Rev. A **40**, 567 (1989).
13. F.W. Byron, Jr., P. Francken, C.J. Joachain, J. Phys. B: At. Mol. Phys. **20**, 5487 (1987).
14. S. Varró, F. Ehlötzky, J. Phys. B: At. Mol. Opt. Phys. **30**, 1061 (1997).